AIAA JOURNAL
Vol. 56, No. 8, August 2018

Technical Notes

Navier–Stokes Equations-Based Aeroelasticity of Supersonic Transport Including Short-Period Oscillations

Guru Guruswamy*
NASA Ames Research Center, Moffett Field, California 94035

DOI: 10.2514/1.J057223

Nomenclature

C_D	=	coefficient of total drag
C_L	=	coefficient of total lift
C_P	=	coefficient of pressure
d_{SP}	=	damping of short-period oscillation
g	=	acceleration due to gravity, ft/s
M	=	Mach number
Q	=	dynamic pressure, lb/ft^2 (or lb/in.^{2})
q	=	pitch rate
S	=	surface area, ft^2
u_0	=	initial velocity, ft/s
α	=	angle of attack, deg
ω_{SP}	=	frequency of short-period oscillation, rad/s

I. Introduction

THERE is renewed interest in developing new supersonic transports [1] after the discontinuation of the Concorde supersonic jet [2], which was mostly limited for flights over transoceanic routes due to the severe noise of the sonic boom. To avoid the sonic boom, more slender configurations, such as the Low Boom Flight Demonstrator configuration [3], are being considered. The aeroelastic characteristics of these new supersonic transports can significantly differ from conventional aircraft. Both rigid and flexible body modes can play a significant role in aeroelastic stability. For unconventional configurations, such as aircraft with forward swept wings, the short-period oscillation (SPO) has been found to significantly impact the aeroelastic response [4]. SPO can occur due to unanticipated events such as gusts, abrupt maneuvering, etc. During the design of the Concorde, the effects of SPO were considered in detail, though its impact is not publically disclosed [5].

Assuring stability of supersonic aircraft, particularly during descent from the supersonic Mach regime to the transonic regime, is critical. An aircraft can deviate from its normal descent trajectory due to coupling between flows and body motions. The effect of SPO needs to be considered in aeroelastic responses. Preliminary studies using quasi-steady aerodynamics show that the presence of SPO can lead to unstable response [6]. The well-established Reynolds-averaged Navier–Stokes (RANS) equations, which are computationally feasible with current supercomputers, have been in use for aeroelastic computations for the last three decades [7]. Recently, such efforts have begun to include trajectory motions [8]; for instance, the effect of phugoid motion on stability is studied in [9] using the RANS equations.

In this Note, the effect of SPO on aeroelastic responses of a typical supersonic transport is studied.

II. Short-Period Oscillation Equations of Motion

Following the derivations of [10], the frequency of short-period oscillations is defined as

$$\omega_{sp} = \frac{M_q Z_\alpha}{u_0} \tag{1}$$

where $M_q = C_{mq} lQSc/(2u_0 I_y)$; $Z_\alpha = u_0 Z_w$; $Z_w = -QS(1/mu_0)(C_{l\alpha} + C_{d0})$; C_{mq} is the pitching moment coefficient with respect to pitch rate q; l is the reference length (root chord); Q is the dynamic pressure; S is the surface area; c is the mean aerodynamic chord; u_0 is the initial velocity; I_y is the moment of inertia about the center of gravity; m is the mass of the aircraft; $C_{l\alpha}$ is the lift coefficient; and C_{d0} is the initial drag coefficient.

The damping is defined as

$$d_{sp} = -0.5\left(\frac{1}{\omega_{sp}}\right)\left(M_\alpha + M_{\dot\alpha} + \frac{Z_\alpha}{u_0}\right) \tag{2}$$

where $M_\alpha = u_0 M_w$; $M_{\dot\alpha} = u_0 M_{\dot w}$; $M_w = C_{m\alpha} QSc/u_0 I_y$; and $M_{\dot w} = C_{m\dot\alpha}(c/2u_0)(QSc/u_0 I_y)$.

These equations are superimposed on the aeroelastic equ ations of motion [11]:

$$[W]\{h\} + [G]\{\ddot h\} + [\dot K]\{h\} = \{F\} \tag{3}$$

where $[W]$, $[G]$, and $[K]$ are the modal mass, damping, and stiffness matrices, respectively. $\{F\}$ and $\{h\}$ are generalized aerodynamic force and displacement vectors, defined as

$$\{F\} = Q[\psi][A]\{c_p\} \tag{4}$$

where ψ is the transpose of the mode shape matrix, $[A]$ is the control area matrix of the computational fluid dynamics (CFD) grid, and $\{c_p\}$ is the average pressure coefficient on the CFD control area. The structural damping G is assumed to be negligible compared to aerodynamic damping. The aerodynamic unsteady load vector $\{F\}$ is computed by solving the RANS equations.

In this work, Eq. (3) is solved using Newmark's time integration method in association with the instantaneous Lagrangian–Eulerian approach (also known as arbitrary Lagrangian–Eulerian) [12], with the aerodynamic data computed by solving the RANS equations [13]. For this work, the RANS equations are numerically solved using the OVERFLOW code [14], which uses the diagonal form of the Beam–Warming central difference algorithm [15], along with the one-equation Spalart–Allmaras turbulence model [16]. An aeroelastic solution module is embedded into the OVERFLOW code and validated with wind-tunnel data for a rectangular wing [17]. Figure 1 shows the aeroelastic responses at $M_\infty = 0.90$. Computed results show neutrally stable response at $Q = 1.15$ psi compared to 1.20 as measured in the wind tunnel [17].

Starting from the converged steady-state solution for a given Mach number, time integration of Eq. (3) is solved with and without superposition of SPO applied while the vehicle is experiencing stable aeroelastic oscillation such as limit-cycle oscillation. SPO simulates induced oscillation due to abrupt gust or sudden changes in

Received 15 February 2018; accepted for publication 3 April 2018; published online Open Access 27 April 2018.

*Senior Aerospace Engineer, Computational Physics Branch. Associate Fellow AIAA.

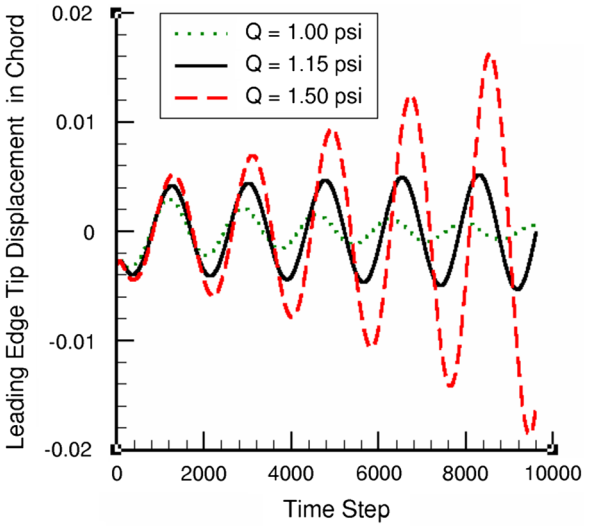

Fig. 1 Dynamic aeroelastic responses at $M_\infty = 0.90$. Measured flutter dynamic pressure $Q = 1.20$ psi, from [17].

maneuvering. The effects of SPO on aeroelastic oscillations are then studied.

III. Results

A generic supersonic transport conceived by NASA Langley Research Center [18] was selected for demonstration because it exists in the public domain. A grid that satisfies engineering requirements, such as in spacing and stretching factors, was selected from [9]. Figure 1 shows alternate grid lines of the surface grid including the wake grid (red), defined by 174 points in the axial direction (x) and 422 points in the circumferential direction (y–z) and near-body section grid at the tail. With H-O topology (H meaning stacked as surfaces in the x direction and O meaning each surface wrapped around the body), the outer boundary surfaces are placed at a distance of about 15 vehicle lengths using 75 grid points. Numerical experiments similar to that reported in [9] were performed for this grid to assess its resolution quality. The selected grid of size $422 \times 174 \times 75$ is found adequate to give acceptable force quantities needed for this work. This grid was validated with wind-tunnel data and the linear theory results as reported in [9]. Figure 3 shows typical flow results at $M_\infty = 0.90$.

By using the structural properties of a typical supersonic transport [18], Eq. (3) is solved at Mach numbers 0.70 and 0.90 with and without superposition of SPO. Figure 6 shows the first bending and torsion modes of the aircraft obtained using a stick model [19].

Based on Eqs. (1) and (2), the short-period oscillatory motion is computed at $M_\infty = 0.70$ and 0.90.

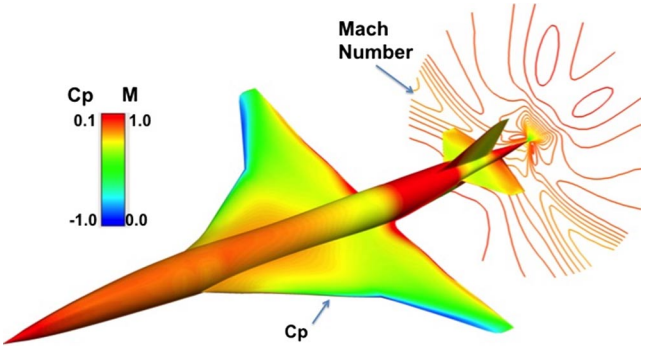

Fig. 3 Surface C_p and tail region Mach number distributions at $M_\infty = 0.90, \alpha = 5$ deg.

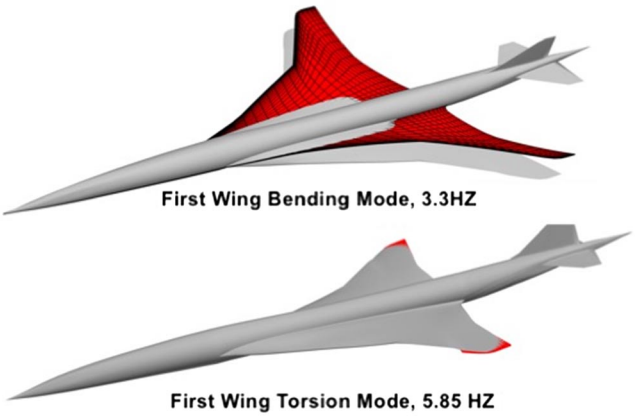

Fig. 4 First two modes and frequencies.

Figure 5 shows the damped motion of duration 0.08 s for $M_\infty = 0.90$ with assumed initial angle attack of 3 deg.

Computations are first made by solving Eq. (3) without SPO. A well-established time integration method [11] is used to solve Eq. (3). It is found that near-limit-cycle oscillations occur at $Q = 130$ and 80 lb/ft^2 at $M_\infty = 0.70$ and 0.90, respectively. The SPO is superimposed on this response at a time of 0.5 s. Figure 6 shows responses with and without SPO for $M_\infty = 0.70$. Without SPO, the limit cycle response is mostly close to the twist mode. With SPO, the response is initially magnified but finally reaches a neutrally stable condition. Figure 7 shows responses of the first generalized displacement with and without SPO for $M_\infty = 0.90$. The response without SPO is neutrally stable with contributions from both bending and torsion modes. The addition of SPO finally leads to a diverging response.

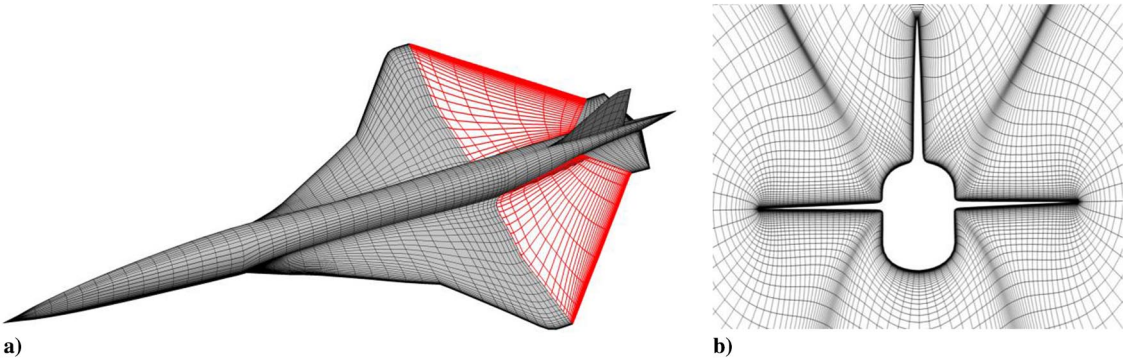

Fig. 2 Grids: a) surface and wake (red) grids of a typical supersonic transport, and b) section grid at the tail.

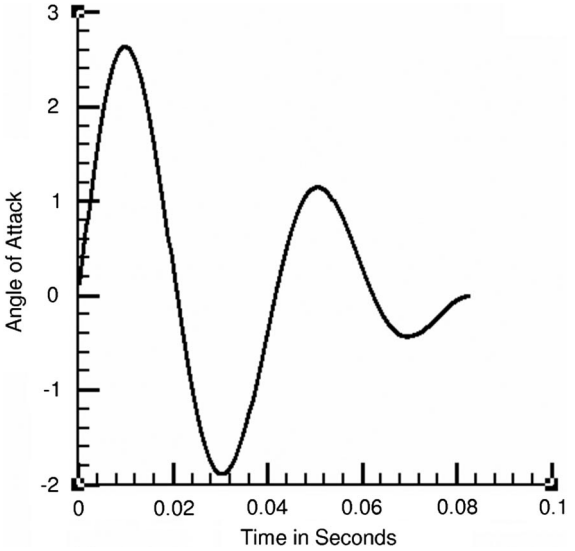

Fig. 5 Short-period motion at $M_\infty = 0.90$.

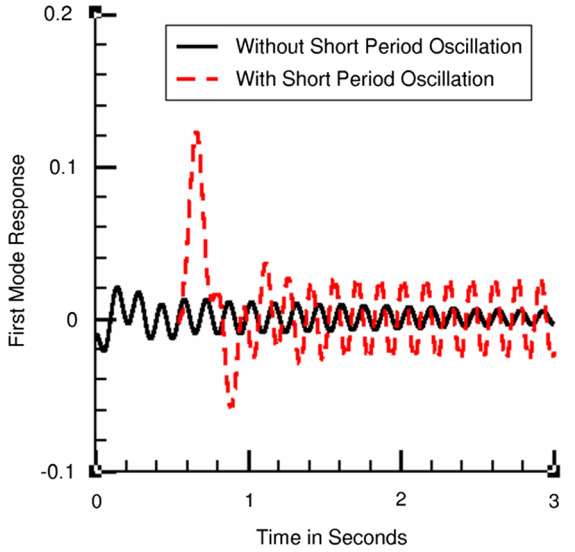

Fig 6 Responses with and without SPO at $M_\infty = 0.70$.

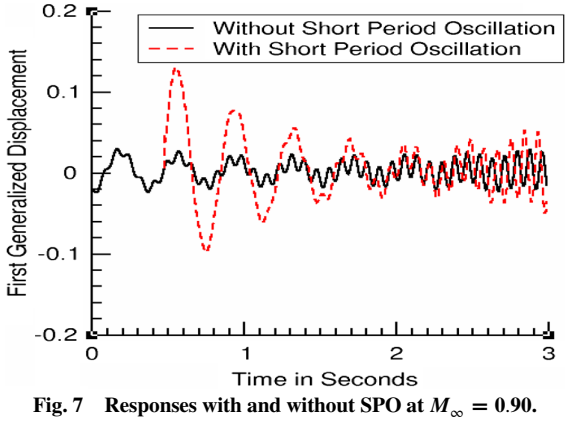

Fig. 7 Responses with and without SPO at $M_\infty = 0.90$.

IV. Conclusions

This work presents a complete time-accurate procedure based on the Reynolds-averaged Navier–Stokes (RANS) equations to compute responses including short-period oscillations (SPO). The procedure presented in this Note will help in the design of highly slender, next-generation supersonic transports. The fully time-accurate approach presented here can be used to determine if aeroelastic oscillations are initiated from short-period oscillations. Present computations show that SPO can make a system less stable in the transonic regime. Demonstration of use of the RANS equations for advanced aeroelastic applications as presented in this Note can help to expand the scope of new computational fluid dynamics codes such as FUN3D [20] and LAVA [21] that are under development based on modified RANS algorithms mostly for rigid configurations. Future work involves modeling active controls [22] to alleviate aeroelastic instabilities due to SPO.

Acknowledgments

This work was partially supported under applied research activity of the NASA Advanced Supercomputing Division, Ames Research Center.

References

[1] "NASA Begins Work to Build Quieter Supersonic Passenger Jet," NASA, Feb. 2016, https://www.nasa.gov/press-release/nasa-begins-work-to-build-a-quieter-supersonic-passenger-jet [retrieved April 2018].

[2] Lawless, J., "Final Concorde Flight Lands at Heathrow," *Washington Post*, Oct. 2003, http://www.washingtonpost.com/wp-dyn/articles/A11477-2003Oct24.html [accessed 30 Oct. 2017].

[3] Ordaz, I., Geiselhart, K., and Fenbert, J. W., "Conceptual Design of Low Boom Supersonic Aircraft with Flight Trim Requirement," *32nd AIAA Applied Aerodynamics Conference*, AIAA Paper 2014-2141, June 2014.

[4] Miller, G. D., Wykes, J. H., and Brosnan, M. J., "Rigid-Body Structural Mode Coupling on a Forward Swept Wing Aircraft," *Journal of Aircraft*, Vol. 20, No. 8, Aug. 1983, pp. 696–702. doi:10.2514/3.44931

[5] Broadbent, E. G., Zbrozek, J. K., and Huntley, E., "A Study of Dynamic Aeroelastic Effects on the Stability Control and Gust Response of a Slender Delta Aircraft," Aeronautical Research Council, R&M No. 3690, London, U.K., 1972.

[6] Baldelli, D. H., Chen, P. C., and Panza, J., "Unified Aeroelastic and Flight Dynamic Formulation via Rational Function Approximations," *Journal of Aircraft*, Vol. 43, No. 3, May–June 2006, pp. 763–772. doi:10.2514/1.16620

[7] Guruswamy, G. P., "Computational Aeroelasticity," *The Standard Handbook for Aerospace Engineers*, McGraw–Hill, New York, Feb. 2018, pp. 273–285.

[8] Guruswamy, G. P., "Time Accurate Coupling of 3-DOF Parachute System with Navier–Stokes Equations," *Journal of Spacecraft and Rockets*, Vol. 54, No. 6, Nov.–Dec. 2017, pp. 1278–1283. doi:10.2514/1.A33835

[9] Guruswamy, G. P., "Phugoid Motion Simulation of a Supersonic Transport Using Navier–Stokes Equations," *AIAA Journal*, advance online publication, April 2018. doi:10.2514/1.J056653

[10] Nelson, C. R., *Flight Stability and Automatic Control*, 2nd ed., WCB/McGraw–Hill, New York, 1998, Sec. 4.5.

[11] Guruswamy, G. P., "Computational-Fluid-Dynamics and Computational-Structural-Dynamics Based Time-Accurate Aeroelasticity of Helicopter Blades," *Journal of Aircraft*, Vol. 47, No. 3, May–June 2010, pp. 858–863. doi:10.2514/1.45744

[12] Guruswamy, G. P., "Time-Accurate Aeroelastic Computations of a Full Helicopter Model Using the Navier–Stokes Equations," *International Journal of Aerospace Innovations*, Vol. 5, Nos. 3–4, Dec. 2013, pp. 73–82. doi:10.1260/1757-2258.5.3-4.73

[13] Peyret, R., and Viviand, H., "Computation of Viscous Compressible Flows Based on Navier–Stokes Equations," AGARD Rept. AG-212, Neuilly sur Seine, France, 1975.

[14] Nichols, R. H., Tramel, R. W., and Buning, P. G., "Solver and Turbulence Model Upgrades to OVERFLOW 2 for Unsteady and High-Speed Applications," *AIAA 36th Fluid Dynamics Conference*, AIAA Paper 2006-2824, June 2006.

[15] Beam, R. M., and Warming, R. F., "An Implicit Factored Scheme for the Compressible Navier–Stokes Equations," *AIAA Journal*, Vol. 16, No. 4, 1978, pp. 393–402. doi:10.2514/3.60901

[16] Spalart, P. R., and Allmaras, S., "A One-Equation Turbulence Model for Aerodynamic Flows," *30th Aerospace Sciences Meeting and Exhibit*, AIAA Paper 1992-0439, 1992.

[17] Dogget, R. V., Rainey, A. G., and Morgan, H. G., "An Experimental Investigation on Transonic Flutter Characteristics," NASA TMX-79, Nov. 1959.

[18] Raney, D. L., Jackson, E. B., and Buttrill, C. S., "Simulation Studies of Impact of Aeroelastic Characteristics on Flying Qualities of a High Speed Civil Transport," NASA TP 2002-211943, Oct. 2002.

[19] Guruswamy, G. P., "Coupled Finite-Difference/Finite-Element Approach for Wing-Body Aeroelasticity," *4th Symposium on Multidisciplinary Analysis and Optimization*, AIAA Paper 1992-4680, Sept. 1992.

[20] Chawalowski, P., and Heeg, J., "FUN3D Analyses in Support of the Second Aeroelastic Prediction Workshop," *34th AIAA Applied Aerodynamics Conference*, AIAA Paper 2016-3122, 2016.

[21] Kiris, C. C., Barad, M. F., Housman, J. A., Sozer, E., Brehm, C., and Moini-Yekta, S., "The LAVA Computational Fluid Dynamics Solver," *52nd Aerospace Sciences Meeting*, AIAA Paper 2014-0070, Jan. 2014.

[22] Guruswamy, G. P., "Integrated Approach for Active Coupling of Structures and Fluids," *AIAA Journal*, Vol. 27, No. 6, June 1989, pp. 788–793.
doi:10.2514/3.10179

S. Fu
Associate Editor